Oncology Research, Vol. 28, pp. 579–590
Printed in the USA.

0965-0407/21 $90.00 + .00
DOI: https://doi.org/10.3727/096504020X15942028641011
E-ISSN 1555-3906
www.cognizantcommunication.com

IL-24-Armed Oncolytic Vaccinia Virus Exerts Potent Antitumor Effects via Multiple Pathways in Colorectal Cancer

Lili Deng,*[1] Xue Yang,†[1] Jun Fan,* Yuedi Ding,* Ying Peng,* Dong Xu,* Biao Huang,*‡ and Zhigang Hu†

*NHC Key Laboratory of Nuclear Medicine, Jiangsu Key Laboratory of Molecular Nuclear Medicine, Jiangsu Institute of Nuclear Medicine, Wuxi, P.R. China
†Wuxi Children's Hospital, Wuxi People's Hospital Affiliated to Nanjing Medical University, Wuxi, P.R. China
‡School of Life Science, Zhejiang Sci-Tech University, Hangzhou, P.R. China

Colorectal cancer is an aggressive malignancy for which there are limited treatment options. Oncolytic vaccinia virus is being developed as a novel strategy for cancer therapy. Arming vaccinia virus with immunostimulatory cytokines can enhance the tumor cell-specific replication and antitumor efficacy. Interleukin-24 (IL-24) is an important immune mediator, as well as a broad-spectrum tumor suppressor. We constructed a targeted vaccinia virus of Guang9 strain harboring IL-24 (VG9-IL-24) to evaluate its antitumor effects. In vitro, VG9-IL-24 induced an increased number of apoptotic cells and blocked colorectal cancer cells in the G_2/M phase of the cell cycle. VG9-IL-24 induced apoptosis in colorectal cancer cells via multiple apoptotic signaling pathways. In vivo, VG9-IL-24 significantly inhibited the tumor growth and prolonged the survival both in human and murine colorectal cancer models. In addition, VG9-IL-24 stimulated multiple antitumor immune responses and direct bystander antitumor activity. Our results indicate that VG9-IL-24 can inhibit the growth of colorectal cancer tumor by inducing oncolysis and apoptosis as well as stimulating the antitumor immune effects. These findings indicate that VG9-IL-24 may exert a potential therapeutic strategy for combating colorectal cancer.

Key words: Oncolytic vaccinia virus; Interleukin-24 (IL-24); Colorectal cancer (CRC); Immunotherapy; Apoptosis

INTRODUCTION

Colorectal cancer (CRC) is an aggressive malignancy, making it the fourth most diagnosed cancer and the second leading cause of cancer death in the US[1]. Despite recent improvements in traditional approaches for enhanced survival of early stage disease, patients with recurring or late stage disease are still not considerably curative. Therefore, efficient treatment strategies with multiple mechanisms of action are urgently required for patients suffering from primary colorectal cancer and metastases.

A wide variety of preclinical studies or clinical trials have employed oncolytic viruses as a novel strategy for cancer therapy[2–5]. Unlike traditional cancer therapy, oncolytic viruses selectively infect, replicate within and lyse tumor cells, and spread to neighboring tumor cells in successive rounds of replication[6,7]. Additionally, oncolytic viruses also generate antitumor immunity that eradicates metastasized tumor cells with minimum harm to the normal tissue[8]. Such effects have been under investigation on a number of viruses, including adenovirus, herpes simplex virus, Newcastle disease virus, and vaccinia virus[9–12]. Studies have demonstrated that these oncolytic viruses may have potential for CRC therapy[13–15].

Among various oncolytic viruses, vaccinia virus has some unique characteristics, such as large transgene-encoding capacity, efficient foreign gene expression using its own enzyme systems, intravenous stability, and well-established safety in humans as a live vaccine. To promote its efficacious oncolytic potency and tumor selectivity, numerous therapeutic genes, cytokines, and immunostimulatory molecules have been inserted into the thymidine kinase (TK) gene region of vaccinia virus[16–19]. In our previous study, we engineered an oncolytic vaccinia virus of Tian Tan strain Guang9 (VG9) expressing granulocyte–macrophage colony-stimulating factor (GM-CSF) and

[1]These authors provided equal contribution to this work.
Address correspondence to Zhigang Hu, Wuxi Children's Hospital, Wuxi People's Hospital Affiliated to Nanjing Medical University, Qingyang Road #299-1, Wuxi, Jiangsu 214023, P.R. China. Tel: +(86)051085350227; E-mail: jswxhzg@163.com *or* Biao Huang, Zhejiang Sci-Tech University, Xiasha District, Street 2, #926, Hangzhou, Zhejiang 310018, P.R. China. Tel: +(86)057186843187; E-mail: huangbiao@jsinm.org

have demonstrated its efficacious antitumor effects in a murine melanoma model[20]. In this study, we find another promising cytokine, interleukin-24 (IL-24), which is an important immune mediator, as well as a broad-spectrum tumor suppressor[21], exerting potent antitumor effects on CRC. We inserted *IL-24* gene into the TK locus of VG9 (VG9-IL-24) and evaluated the antitumor effects both in vitro and in vivo.

MATERIALS AND METHODS

Cell Lines

The murine colorectal carcinoma cell line CT26, human colorectal carcinoma cell line HCT116, human colorectal adenocarcinoma cell line HT-29, human ileocecal colorectal adenocarcinoma cell line HCT-8, and murine breast cancer cell line 4T1 were purchased from the Cell Bank of Shanghai Institute for Biological Sciences of the Chinese Academy of Sciences (Shanghai, China). African green monkey kidney epithelial cell line BSC-40 was purchased from the American Type Culture Collection (ATCC, Manassas, VA, USA). All cell lines were cultured under the conditions suggested by the ATCC.

Recombinant Vaccinia Virus VG9-IL-24

VG9-IL-24 was constructed via disruption of the viral TK gene region based on vaccinia strain VG9, which was obtained from the National Institutes for Food and Drug Control (Beijing, China). VG9-EGFP was constructed and conserved in our laboratory[22]. The generation of recombinant vaccinia viruses based on *gpt* selection was previously described in detail[20,22]. All recombinant vaccinia viruses were purified in sucrose gradient, and virus stocks were titrated on BSC-40 cells by plaque assay.

IL-24 Expression

The various CRC cell lines grown in 12-well plates were infected with 0.1 multiplicity of infection (MOI) of VG9-IL-24 for 48 h. IL-24 protein was analyzed by Western blot. Supernatants and lysates were collected, and IL-24 levels were quantitatively determined by the ELISA kit (R&D Systems Inc., Minneapolis, MN, USA) according to the manufacturer's manual.

In Vitro Cytotoxicity

Cells seeded in 96-well plates were infected with different concentrations (0.01, 0.1, 1, and 10 MOI) of the virus for 72 h or infected with 0.1 MOI of the virus for different times (24, 48, and 72 h). Cell viability was analyzed by the MTT assay.

Cell Apoptosis and Cell Cycle Detection

Morphological characteristics of apoptotic cells were observed by Hoechst 33258 staining. CRC cells infected with VG9-IL-24, VG9-EGFP, or PBS for 24 h were incubated with Hoechst 33258 (Beyotime Biotechnology, Shanghai, China) for 30 min. The apoptotic morphological changes of cells were observed under an Olympus IX51 fluorescence microscope (Olympus Corporation, Tokyo, Japan) immediately.

Apoptosis was further quantified by flow cytometric analysis using the Annexin-V–FITC/Propidium Iodide (PI) Apoptosis Detection kit (Roche Applied Science, Penzburg, Germany). HCT116 cells were infected with VG9-IL-24, VG9-EGFP, or PBS for 48 h, and apoptotic cells were detected according to the manufacturer's instructions using BD FACSCalibur (BD Biosciences, Mountain View, CA, USA).

For cell cycle detection, HCT116 cells seeded in six-well plates were infected with VG9-IL-24, VG9-EGFP, or PBS for 48 h and then fixed in 70% cold ethanol overnight at −20°C. Cells were washed with PBS and resuspended in 50 μg/ml of PI solution. After incubation for 30 min in the dark at 37°C, the treated cells were analyzed by flow cytometry (BD FACSCalibur, BD Biosciences). The percentages of G_0/G_1, S, and G_2/M stage cells were quantified using Flow Jo Software (Tristar, Mountain View, CA, USA).

Western Blotting

HCT116 cells seeded in a six-well plate were PBS treated or infected with viruses for 48 h, and the cells were harvested and lysed with RIPA lysis buffer containing protease and phosphatase inhibitors. Protein concentration was measured using the BCA protein assay kit (Thermo Fisher Scientific, Carlsbad, CA, USA), and equal amounts of proteins from each sample were separated using SDS-PAGE and transferred to polyvinylide difluoride membrane (Thermo Fisher Scientific). The antibodies against PARP, PKR, p38 MAPK, p-p38 MAPK (Thr180/Tyr182), JNK, p-JNKs (Thr183/Thr183/Thr221), STAT3, and p-STAT3 (Tyr705) were purchased from Cell Signaling Technology (Danvers, MA, USA), ERK1/2, p-ERK1 (Thr202/Tyr204)/ERK2 (Thr185/Tyr187), Bad, Bcl-xL, and Bcl-2 were purchased from Beyotime Institute of Biotechnology (China). β-Actin was obtained from Santa Cruz Biotechnology (Santa Cruz, CA, USA). Immunoreactive bands were visualized with chemiluminescence using ECL Western blot detection reagents (Santa Cruz Biotechnology).

Animal Studies

The animal experiment was approved by the Institutional Animal Care and Use Committees (IACUC) of Jiangsu Institute of Nuclear Medicine (JSINM2010007). Female nude BALB/c mice (5–6 weeks old) and BALB/c immune-competent mice (6 weeks old) were purchased from Shanghai Laboratory Animals Center (SLAC; Shanghai, China). All procedures were performed in accordance with the National Institutes of Health guide for the care and use of laboratory animals.

To establish the human HCT116 colorectal carcinoma model, athymic nude mice were injected subcutaneously with 5×10^6 HCT116 cells. For the murine CT26 colorectal carcinoma model, 5×10^5 CT26 cells were injected subcutaneously into the right flanks of BALB/c immune-competent mice.

When tumors reached the size of 3–5 mm in diameter, mice were randomly divided into three groups and were intratumorally injected with PBS (control group), and 10^7 PFU of VG9-IL-24 or VG9-EGFP. Tumor size was measured every other day by Vernier calipers, and the tumor volume was calculated as $[(\text{width})^2\times\text{length}]\times0.52$[23]. Mice were euthanized when tumors reached 16 mm in any dimension or at the termination of the experiment, and Kaplan–Meier survival curves were plotted.

The cured immune-competent mice were rechallenged by subcutaneous injection of CT26 cells (5×10^5) or 4T1 cells (1×10^6) into the contralateral side; naive mice (no tumor bearing or virus treated) were also injected subcutaneously with 5×10^5 CT26 cells in the same flank as controls. Tumor growth and survival were followed over time.

The bilateral tumor model was established by subcutaneous injection of CT26 cells into both flanks of female BALB/c immune-competent mice (5×10^5 to the right flank and 1×10^5 to the left flank). When the right flank tumor developed to 3–5 mm in diameter, 10^7 PFU of VG9-IL-24 or VG9-EGFP or PBS was intratumorally injected into the right flanks. The tumors on the left flanks were not injected with virus. Tumor growth was measured over time.

Virus Replication In Vivo

To assess virus replication in vivo, mice were intraperitoneally injected with 1×10^7 PFU VG9-EGFP or VG9-IL-24. Whole sections of brain, lung, liver, spleen, kidney, and tumor were collected and homogenized after infection for 5 days, and a standard plaque assay was performed on BSC-40 cells.

Hematoxylin and Eosin (H&E) and Immunohistochemical Staining

Tumor tissues from each group were harvested and fixed in 10% neutral formalin. After conventional paraffin embedding, H&E staining, and immunohistochemical staining were performed according to standard protocols. For immunohistochemical analysis, sections were incubated with Ki-67 (1:100; Novus Biologicals, Centennial, CO, USA), vascular endothelial growth factor (VEGF), CD34, and IL-24 antibodies (1:50; Abcam, Cambridge, UK). Images were taken with a microscope (magnification, 400×).

CTL Study

Spleen cells were respectively harvested from tumor-bearing mice treated with viruses or PBS to evaluate the killing effect of cytotoxic lymphocyte (CTL) on CT26 cells. CTL activity was measured by fluorescence-activated cell sorting using the ACT1 assay (Cell Technology, Mountain View, CA, USA). Briefly, CT26 cells were incubated with the cell-tracking dye carboxyfluorescein diacetate succinimidyl ester (CFSE) and cultured with splenocytes at various ratios (10:1, 20:1, 40:1) for 6 h; then amino-actinomycin D (7AAD) stain was added to measure cell death by flow cytometry.

Antibody-Mediated Cytotoxicity Assay

Serum, respectively collected from tumor-bearing mice treated with viruses or PBS after a 14-day postinfection, was added to CT26 or 4T1 cells at a concentration of 10% in 96-well plates. After 48 h, cell viability was measured by ADCC Reporter Bioassay (Complete Kit; Promega, San Luis Obispo, CA, USA) according to the manufacturer's instructions.

Determination of Cytokines

After injection of viruses or PBS for 7 days, serum was respectively obtained from the VG9-IL-24, VG9-EGFP, or control group. Cytokine levels of IFN-γ, TNF-α, IL-4, and IL-6 were measured by the ELISA kit (eBioscience, San Diego, CA, USA).

Statistical Analysis

Statistical analysis was performed by SPSS 19.0 software (SPSS Statistics, Inc., Chicago, IL, USA). Data are presented as mean ± standard deviation (SD). One-way ANOVA analyses were employed to compare multiple groups, followed by Tukey's test for two groups. Survival was analyzed by Kaplan–Meier curves, and differences between curves were assessed using the log-rank test.

RESULTS

IL-24 Expression in CRC Cell Lines

All CRC cell lines treated with VG9-IL-24 expressed IL-24 protein (Fig. 1A). ELISA results further confirmed that the concentrations of IL-24 protein from all CRC cells treated with VG9-IL-24 was elevated (Fig. 1B). No IL-24 production was detected in cells treated with VG9-EGFP or PBS (data not shown). The results suggested that VG9-IL-24 was able to replicate in various CRC cells, and the harboring *IL-24* gene could be overexpressed. The highest level of IL-24 protein was observed in CT26 cells, indicating the strongest replication ability of VG9-IL-24 in CT26 cells.

Cytotoxicity of VG9-IL-24 in CRC Cell Lines

CRC cell lines exhibited significant sensitivity to VG9-IL-24-induced cytotoxicity, which killed CRC cells in a dose- and time-dependent manner (Fig. 1C, D). Although differences were observed between cell lines

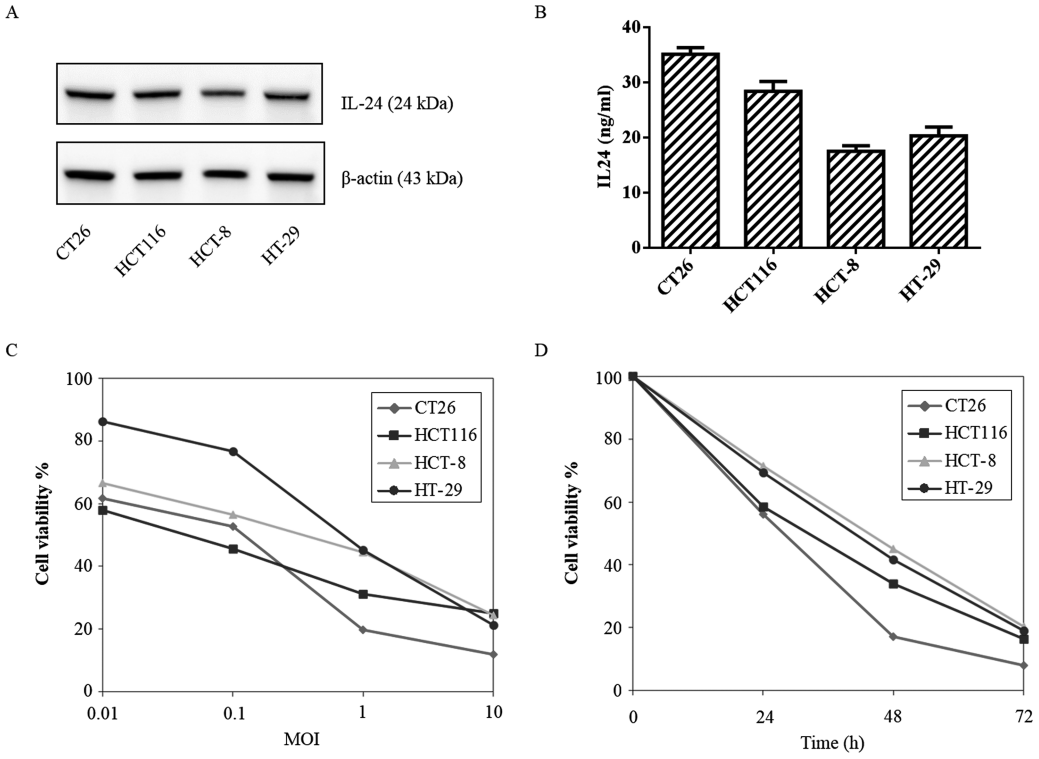

Figure 1. Characterization of vaccinia virus of Guang9 strain harboring IL-24 (VG9-IL-24). (A) Western blot analysis of IL-24 protein from different colorectal cancer cell lines treated with VG9-IL-24 at 0.1 MOI for 48 h. (B) Supernatants and lysates from colorectal cancer cell lines treated with VG9-IL-24 at 0.1 MOI for 48 h, and IL-24 concentrations were quantified by ELISA. Each bar represents the mean ± SD ($n = 3$). (C) Cytotoxicity effect of VG9-IL-24 with different MOIs on colorectal cancer cells after infection for 72 h. (D) Cytotoxicity effect of VG9-IL-24 (0.1 MOI) on colorectal cancer cells after infection for different times.

at a low MOI, all four CRC cell lines exhibited obvious cytotoxicity after virus infection. VG9-IL-24 showed the strongest cytotoxicity in CT26 cells with only 7.96% cell survival at 10 MOI after 72 h of infection.

VG9-IL-24 Induces Apoptosis in CRC Cell Lines

As shown in Figure 2A, all tested CRC cell lines treated with VG9-IL-24 exhibited greater nuclear fragmentation, chromatin clumping, and apoptotic body formation. Flow cytometry results showed that the percentages of apoptotic cells were 22.94 ± 1.83%, 97.98 ± 1.31%, and 49.86 ± 2.02% for PBS, VG9-IL-24, and VG9-EGFP, respectively (Fig. 2B). The ability of VG9-IL-24 in inducing apoptosis was to a greater degree compared with VG9-EGFP ($p < 0.01$).

Cell cycle analysis indicated that VG9-IL-24 induced cell cycle arrest at the G_2/M phase. Compared with the PBS and VG9-EGFP groups, VG9-IL-24 treatment resulted in a higher proportion of apoptotic cells in the G_2/M phase, accompanied with a decrease in the number of cells in the G_1 and S phases (Fig. 2C).

The expression levels of apoptosis-related proteins were determined by Western blot (Fig. 3). Cleaved PARP and Bad were significantly increased, while Bcl-xL expression was decreased. However, the expression level of Bcl-2 showed no significant change. Signal pathways results showed that VG9-IL-24 treatment increased the level of PKR, which led to subsequent phosphorylation of downstream targets p38MAPK (Thr180/Tyr182). JNK, as a proapoptotic member of MAPK family, was also activated by phosphorylation, whereas phosphorylation was decreased in ERK, which is considered as an antiapoptotic member of the MAPK family. In addition, VG9-IL-24 treatment also decreased the phosphorylation level of STAT3.

Virus Replication In Vivo

The in vivo replication of VG9-IL-24 in tumors and normal organ tissues (brain, spleen, lung, liver, and kidney) was assessed 5 days postinfection, and viral yield was calculated per milligram of tissue (Table 1). Both VG9-EGFP and VG9-IL-24 produced a lower viral yield in normal organ tissues, while they were infective in tumors.

Antitumor Effect of VG9-IL-24 in Nude Mice

HCT116 xenograft tumors in PBS-treated mice grew progressively, while tumors in virus-treated mice were notably suppressed (Fig. 4A). VG9-IL-24 exhibited more

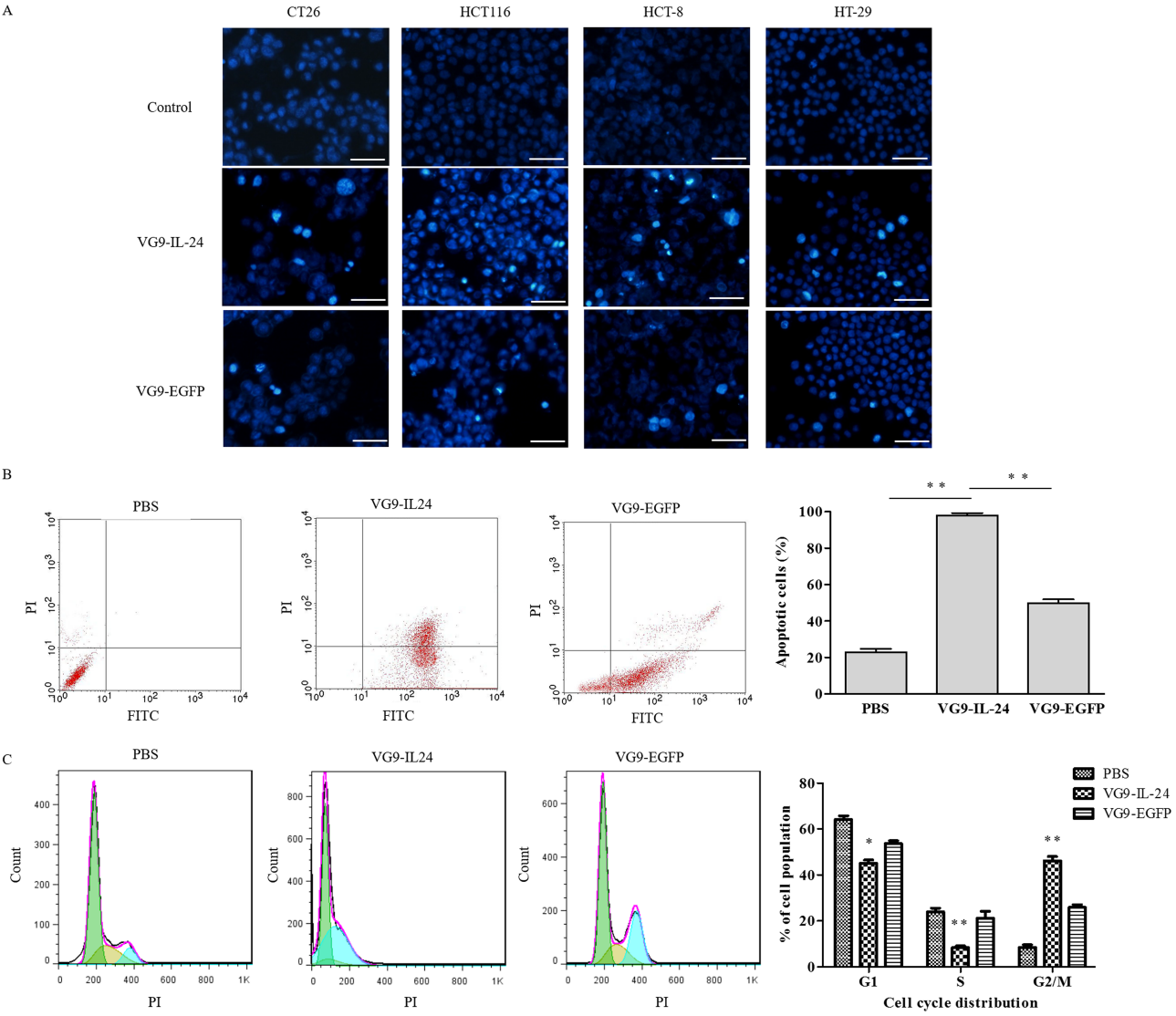

Figure 2. VG9-IL-24 induced apoptosis in colorectal cancer cell. (A) Cell apoptotic staining by Hoechst 33258. Colorectal cancer cell lines CT26, HCT116, HCT-8, and HT-29 treated with PBS, VG9-IL-24, and VG9-EGFP were incubated with Hoechst 33258 for 30 min, then observed nuclear swelling or karyorrhexis with fluorescence microscope. Scale bar: 50 μm. (B) Annexin V and propidium iodide (PI) double staining assay. HCT116 cells treated with PBS, VG9-IL-24, or VG9-EGFP were harvested after 48 h and stained with FITC-labeled annexin V and PI and immediately analyzed by flow cytometry. The percentage of apoptotic cells was calculated with CellQuest software. (C) Cell cycle analysis by PI single staining. HCT116 cells were treated with PBS, VG9-IL-24, or VG9-EGFP for 48 h, and then the distribution of cells in different phases of cell cycle was analyzed by flow cytometry after PI staining. The percentage of cell cycle phases was analyzed by Flow Jo software. Each bar represents the mean ± SD ($n = 3$). *$p < 0.05$, **$p < 0.01$.

strong ability to inhibit tumor growth compared with VG9-EGFP. In addition, survival analysis also showed that tumor development was significantly delayed in VG9-IL-24-treated mice with survival extended until the experiment was finished (50 days); however, all control mice developed tumor and died within 28 days (Fig. 4B).

H&E staining showed that apparent karyopyknosis, cracking, and a large quantity of bubbles between tissues were observed in the VG9-IL-24 group, indicating that VG9-IL-24 treatment caused more severe cytopathic effects in tumor tissues (Fig. 4C). Immunohistochemical analysis for Ki-67 showed that the percent of positive Ki-67 in the control, VG9-EGFP, and VG9-IL-24 groups was 96%, 62%, and 23%, respectively, indicating that VG9-IL-24 significantly inhibited the proliferation of tumor cells. The expression of VEGF protein was apparently decreased in vesicles of tumors infected with VG9-IL-24. CD34 expression in the VG9-IL-24 group was also lower compared with the PBS or VG9-EGFP group

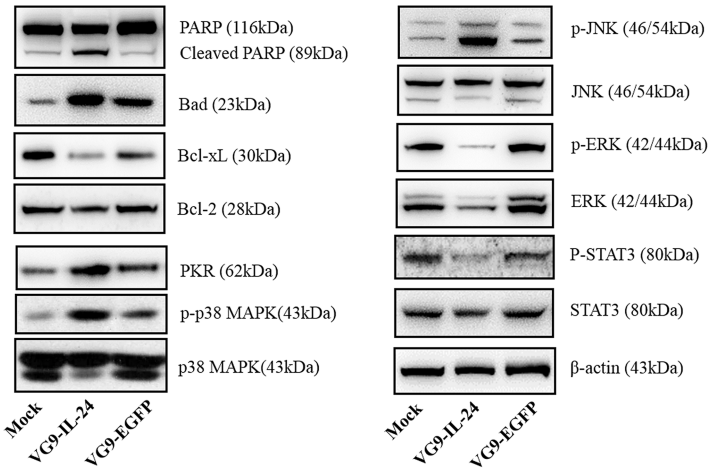

Figure 3. Signaling pathways induced by VG9-IL-24. HCT116 cells treated with PBS, VG9-IL-24, or VG9-EGFP for 48 h were harvested, lysed, separated by SDS-PAGE, and examined by Western blot analysis for PARP, Bad, Bcl-xL, Bcl-2, PKR, p-p38, p38, p-JNK, JNK, p-ERK1/2, ERK1/2, p-STAT3, and STAT3. β-Actin was used as a loading control.

(Fig. 4C). Immunohistochemical staining further confirmed that IL-24 was stably expressed in tumor tissue from the VG9-IL-24-treated group, suggesting that the enhanced antitumor activity of VG9-IL-24 was probably duo to the in situ production of IL-24.

Antitumor Effect of VG9-IL-24 in Immune-Competent Mice

As shown in Figure 5A, a single intratumoral injection of virus resulted in evident suppression of tumor growth compared with the control group. The antitumor activity of VG9-IL-24 was much stronger than that of VG9-EGFP with four mice completely healed. Survival advantage was observed in virus-treated mice; the greatest benefit in terms of survival was found in the VG9-IL-24 group, which achieved significantly longer survival compared with the PBS or VG9-EGFP group ($p<0.01$) (Fig. 5B).

Tumor cell rechallenge study showed that all CT26 tumor-burdened mice healed by VG9-IL-24 were resistant to CT26 cells and survived the tumor challenge, whereas mice implanted with 4T1 cells developed tumors (Fig. 5C), indicating that VG9-IL-24 was able to develop systemic antitumoral immunity, and the protection against tumor rechallenge was tumor specific.

In bilateral CT26 murine colorectal tumor model (Fig. 5D), CT26 cells developed rapidly proliferating tumors on bilateral flanks in the control group, while virus injection showed tumor regression on both sides. CT26 tumors injected with VG9-IL-24 grew more slowly compared with VG9-EGFP. Besides, VG9-IL-24-treated mice also showed more profound growth inhibition of non-injected tumors on left flanks. The intratumoral injection of VG9-IL-24 eradicated the primary and distant tumors, which confidently indicated the potent "bystander" antitumor effect of IL-24.

Table 1. Viral Yield in Tumor and Normal Tissues

	VG9-EGFP	VG9-IL-24
Tumor	$10.0\ (8.6–12)\times10^4$	$18.8\ (11.6–20.8)\times10^4$
Brain	18 (0–48)	12 (0–50)
Lung	6 (0–28)	0
Liver	0 (0–20)	0 (0–10)
Spleen	20 (10–80)	12 (0–72)
Kidney	36 (20–70)	30 (0–80)

Values are the median (range) viral yields, PFU/mg tissue on day 5 after injection with VG9-EGFP or VG9-IL-24. Whole sections of normal organ tissues and tumors were collected and homogenized, and a standard plaque assay was performed on BSC-40 cells.

Induction of Antitumor Immunity

CTL killing assay showed that VG9-IL-24 exhibited significant killing activity of CTL on CT26 cells compared to the VG9-EGFP and control group ($p<0.01$). The cell-killing activity was the strongest at a ratio of 40:1 (Fig. 6A). A significant decrease in the viability of CT26 cells was observed with serum from virus-treated mice, while there was no change in 4T1 cell viability upon incubation with serum from any of the treatment groups (Fig. 6B). VG9-IL-24 exhibited stronger cytotoxicity than VG9-EGFP on CT26 cells ($p<0.01$).

As an important immune mediator, IL-24 was able to stimulate various cytokines. As shown in Figure 6C, VG9-IL-24 resulted in the secretion of IFN-γ and IL-6 at high levels, and TNF-α and IL-4 at low levels. All the cytokine levels tested were significantly higher than that in the control or VG9-EGFP group ($p<0.01$, $p<0.05$). To further confirm the presence of IL-24 in serum after VG9-IL-24 treatment, IL-24 concentrations in serum

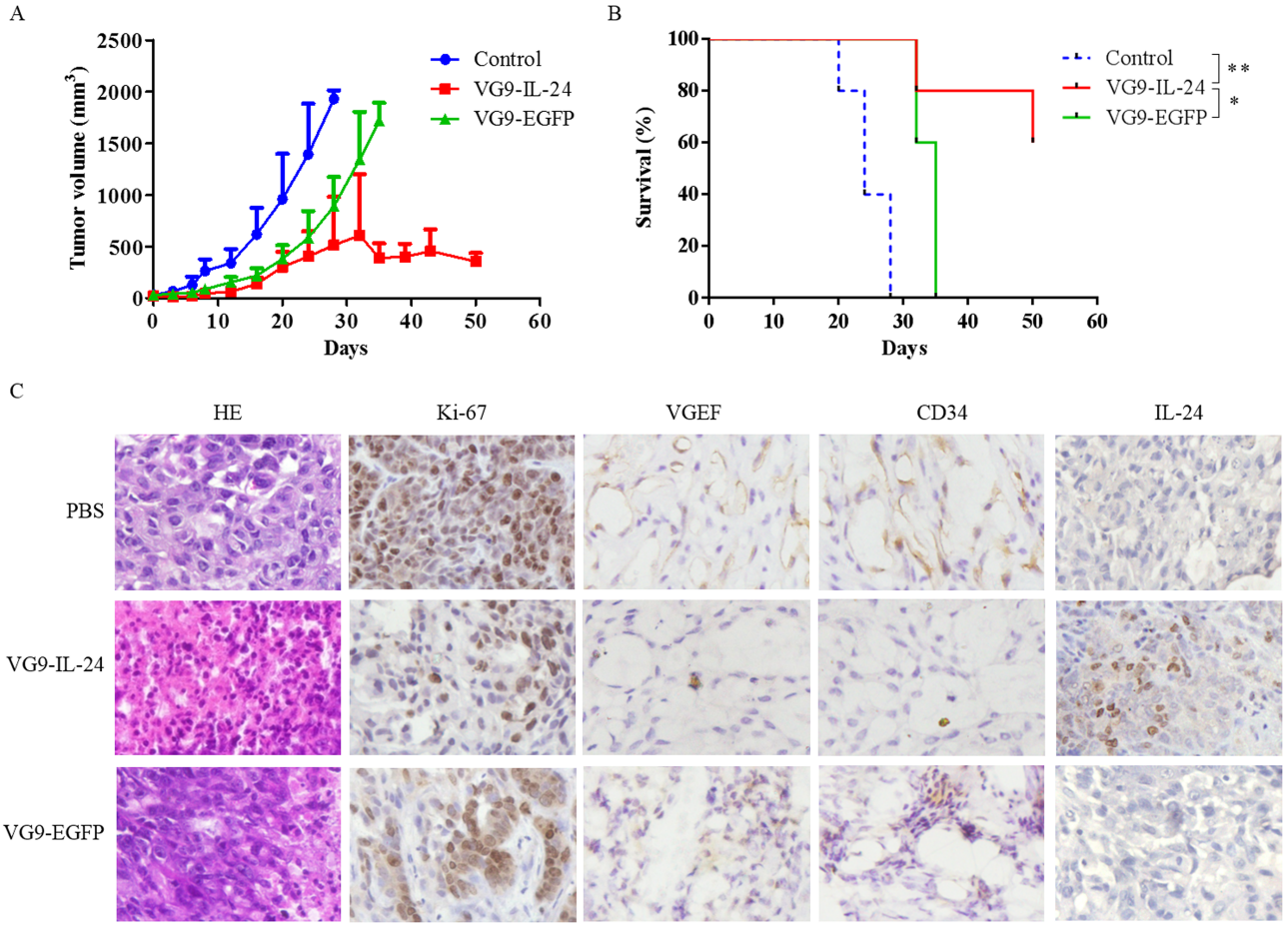

Figure 4. Antitumor effect of VG9-IL-24 in HCT 116 xenograft mouse model. (A) Mean tumor volume in mice treated with PBS (control), VG9-IL-24, or VG9-EGFP. (B) Kaplan–Meier survival curves for tumor-bearing mice treated with PBS, VG9-IL-24, or VG9-EGFP. $n=5$ per group. *$p<0.05$, **$p<0.01$. (C) H&E and immunohistochemical staining of the tumor tissue. Tumors from the mice treated with PBS (control), VG9-IL-24, or VG9-EGFP were harvested, formalin fixed, and paraffin embedded. Sections were subjected to H&E staining and immunohistochemistry for Ki-67 VEGF, CD34, and IL-24. Original magnification: 400×.

harvested at different time points were evaluated by ELISA. As shown in Figure 6D, the level of IL-24 in serum was able to be detected on the second day after initial intratumoral injections of VG9-IL-24 and was continuously elevated, reaching maximum concentration within 7 days. The level of IL-24 was gradually decreased on day 10 but was still able to be detected on day 14. Together, these data implied that VG9-IL-24 induced specific antitumor immunity, which could be enhanced by IL-24 production.

DISCUSSION

Limited by the efficacy of current chemotherapy and aggressive surgery, overall prognosis for CRC, which represents a complex and challenging clinical problem, remains poor, and recurrence rates are still high at present. Therefore, novel strategies for CRC therapy are the need of the hour. Oncolytic virotherapy has emerged as a promising cancer treatment platform in recent years. Owing to direct tumor cell lysis by the virtue of their selective replication in cancer cells, it is possible for oncolytic viruses to treat refractory cancers, like CRC. In this study, we reported a replication-competent vaccinia virus armed with IL-24 (VG9-IL-24) to effectively infect, replicate within, and kill CRC both in vitro and in vivo.

As a novel tumor suppressor cytokine, IL-24 has multifaceted antitumor effects including inducing apoptosis, inhibition of tumor cell invasion and metastasis, antiangiogenic activity, immune modulatory activity, and "bystander" antitumor activity[21,24]. Traditional delivery of IL-24 by liposome or replication-defective adenovirus cannot target tumor cells, which limits its value on cancer gene therapy. Therefore, in this study, we used vaccinia virus as a delivery vector to express the *IL-24* gene. Our study showed that VG9-IL-24 efficiently infected CRC cells, which assured the high expression of IL-24 in cancer cells. ELISA and immunohistochemical analysis further

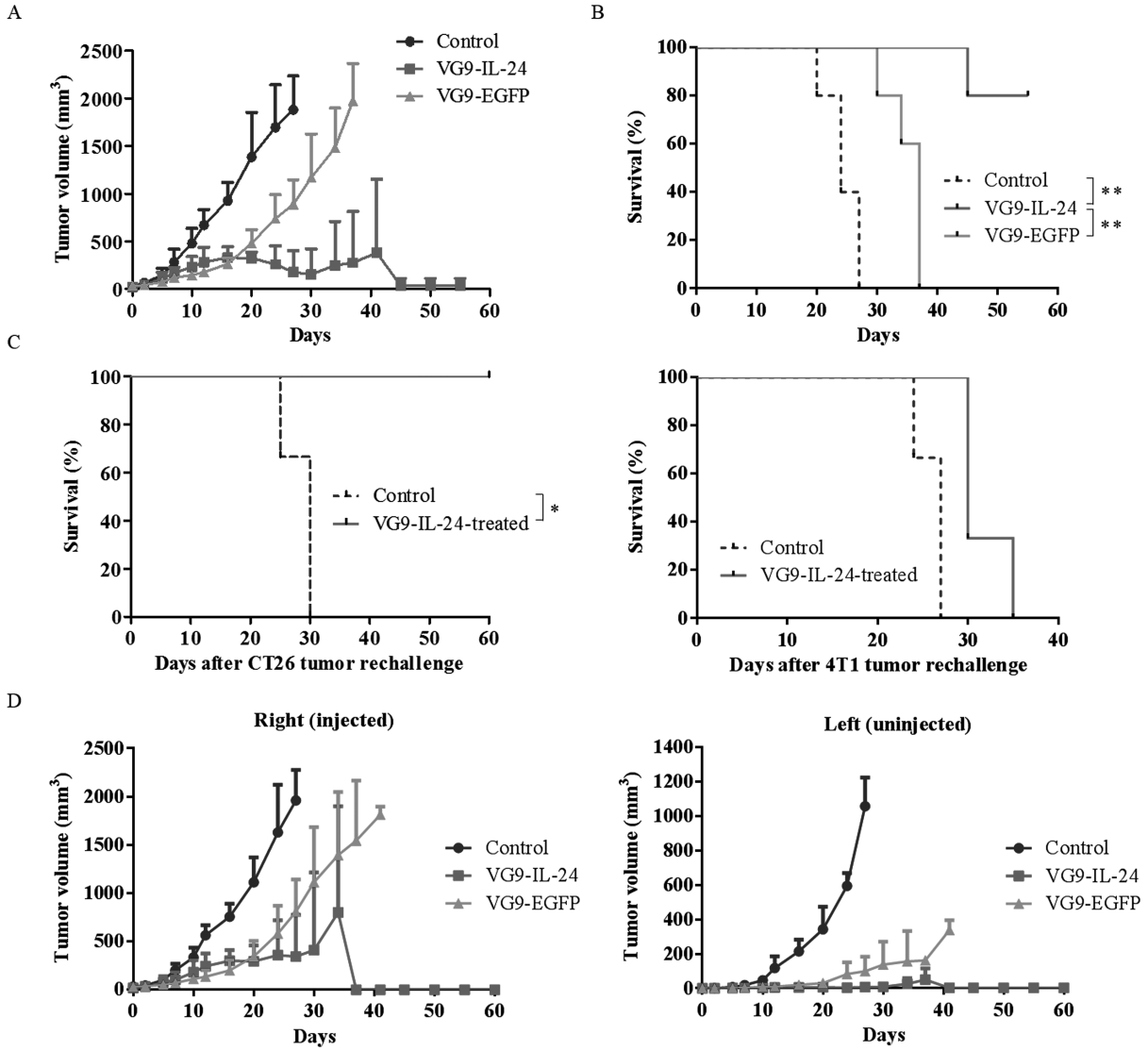

Figure 5. Antitumor effect of VG9-IL-24 in CT26 tumor model. (A) Mean tumor volume in mice treated with PBS (control), VG9-IL-24, or VG9-EGFP. (B) Kaplan–Meier survival curves for tumor-bearing mice treated with PBS, VG9-IL-24, or VG9-EGFP. (C) Kaplan–Meier survival curve of healed CT26 tumor-burdened mice with CT26 tumor and syngeneic 4T1 tumor rechallenge. (D) VG9-IL-24 eradicates primary tumors and inhibits distant tumors in a bilateral intradermal tumor implantation model. Mean volumes of tumors on right flanks of mice injected with PBS (control), VG9-IL-24, or VG9-EGFP and noninjected tumors on left flanks. $n=5$ per group. *$p<0.05$, **$p<0.01$.

demonstrated that VG9-IL-24 sufficiently expressed IL-24 and directly biosynthesized IL-24 protein in tumor cells. Besides, IL-24 was able to be detected in serum, indicating that IL-24 was secreted into the blood from the tumor. All these implied that VG9-IL-24 was able to introduce the IL-24 gene directly into tumors, so that the cytokine was produced in situ, further enhancing the antitumor effects of VG9-IL-24.

There is abundant evidence in the literature that IL-24 can inhibit the proliferation and induce apoptosis in various cancer cells, and its growth-inhibition properties are independent of the status of p53, pRb, and p21[25,26]. In this study, we identified VG9-IL-24 induced in vitro antitumor effects by the suppression of cell growth and induction of cell cycle arrest. VG9-IL-24 promoted apoptosis evidenced by an increase in chromatin condensation, nuclear fragmentation, and the formation of apoptotic bodies in various CRC cell lines via Hoechst staining. Flow cytometric analyses also indicated that VG9-IL-24 induced HCT116 cell cycle arrest at the G_2/M phase. The increase in apoptosis of CRC cells following VG9-IL-24 infection was further confirmed by the appearance of PARP cleavage, a marker of apoptosis induction. Besides, VG9-IL-24 treatment changed the expression of the Bcl-2 family with

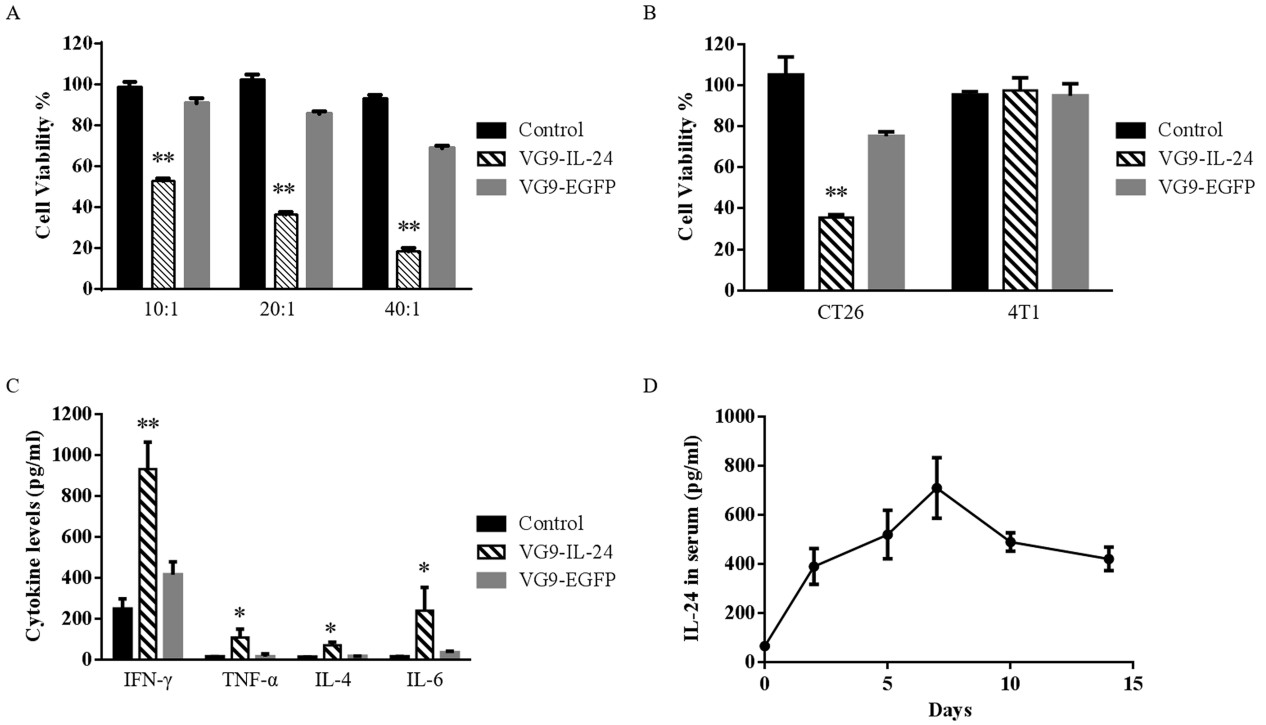

Figure 6. Antitumor immunity induced by VG9-IL-24. (A) Cytotoxic lymphocyte (CTL) killing assay. Viability of CT26 cells cultured with different ratios of splenocytes from CT26 tumor-bearing mice treated with PBS (control group), VG9-IL-24, or VG9-EGFP was measured using the ACT1 assay. (B) Antibody-mediated cytotoxicity assay. Viability of CT26 or 4T1 cells incubated with 10% serum from CT26 tumor-bearing mice treated with PBS (control group), VG9-IL-24, or VG9-EGFP was measured by ADCC Reporter Bioassay. (C) Cytokine levels in serum from tumor-bearing mice treated with PBS (control group), VG9-IL-24, or VG9-EGFP were determined by ELISA kit. (D) The levels of IL-24 expression in serum over time following intratumoral injection of VG9-IL-24 in CT26 tumor-bearing mice. Each bar represents the mean ± SD ($n = 5$). *$p < 0.05$, **$p < 0.01$.

proapoptotic protein Bad upregulation and antiapoptotic protein Bcl-xL downregulation. Changes in the ratio of proapoptotic members and antiapoptotic members of the Bcl-2 family can tip the balance from survival to death. Previous studies have demonstrated that IL-24 treatment resulted in a significant reduction in the levels of specific antiapoptotic proteins in a cancer cell type-specific context[27,28]. In this study, Bcl-xL, not Bcl-2, afforded protection from VG9-IL-24-induced apoptosis in HCT116 cells. The reason why protection is not achieved in all cancer cells with a single functionally similar antiapoptotic protein is not known at present.

The mechanism by which IL-24 induces apoptosis is not well defined, and signaling pathways involved are different and appear to be dependent on tumor types[24]. In this study, we investigated the involvement of PKR, MAPK, and STAT3 signaling pathways in VG9-IL-24-induced apoptosis. Previous studies have found that IL-24-mediated apoptosis is related to PKR, whose role as mediator of antiviral and antitumor responses is known[29,30]. PKR phosphorylates various targets, which play a crucial role in growth control and apoptosis induction, such as eIF-2α, STAT1, STAT3, and p38 MAPK[29]. The MAPK signaling pathway plays important roles in a variety of cellular processes including cell growth, differentiation, development, and apoptosis in response to extracellular stimuli and cellular stress[31]. As members of the MAPK family, p38-MAPK and JNK are known to involve in apoptosis[32,33]. Phosphorylation and activation of p38-MAPK and JNK are involved in cytochrome c release with subsequent caspase activation[34] as well as DNA damage[35]. On the other hand, ERK is considered as an antiapoptotic member of the MAPK family, and its activation can inhibit apoptosis[31]. The oncogenic transcription factor STAT3 is an important member of the signal transducer and activator of transcription family (STAT), which plays crucial roles in regulating a number of diverse biological functions, including cell proliferation, differentiation, apoptosis, immunity, inflammatory response, and angiogenesis[36]. Activation of STAT3 often positively correlates with tumor progression and a poor prognosis. STAT3 is activated by phosphorylation and then forms dimers with other members of the STAT family. The activated STAT3 complex will then translocate from the cytoplasm to the nucleus and bind to the promoters of target genes (including cyclin D1, Bcl-xL, and survivin). Our results showed

that VG9-IL-24 treatment resulted in the activation of PKR, which phosphorylated its downstream target p38 MAPK, subsequently stimulating the MAPK signaling pathway and inhibiting STAT3 phosphorylation, which suppressed its dimerization and nuclear translocation and further induced apoptosis. These results indicated that VG9-IL-24 was able to induce apoptosis in CRC cells via multiple apoptotic signaling pathways.

Tumor angiogenesis plays another important role in the processes of tumor growth, invasion, and metastasis. VEGF, as a tumor-derived growth factor, has a direct effect on vascular endothelial cell growth and vascular permeability and plays a crucial role in tumor angiogenesis[37]. It has been demonstrated that the antiangiogenic effect of IL-24 is more potent and may exert its antiangiogenic activity by a direct or an indirect mechanism or by a combination of both processes[38]. In the present study, immunohistochemical staining demonstrated that VG9-IL-24 treatment significantly downregulated the expression of VEGF and CD34 in the HCT116 xenograft tumors. H&E and Ki-67 detection further showed that VG9-IL-24 did alter the proliferating capacity of HCT116 cells, thus indicating that tumor growth inhibition by VG9-IL-24 was probably attributed to dramatic induction of tumor cell apoptosis as well as its antiangiogenic activity.

In addition to a broad-spectrum tumor suppressor, IL-24 is also an important immune mediator. To investigate whether VG9-IL-24 could induce antitumor immunity, an immune competent mice model (CT26 and 4T1), which has the advantage of an intact immune system, was established in this study. A rechallenge study indicated the ability of VG9-IL-24 to induce a specific and lasting immune response against colorectal tumor. Experiments on the cell killing effect of CTL also showed that VG9-IL-24 could induce CTL to produce a stronger killing effect on CRC cells, but not breast cancer cells, which further confirmed that vaccinia oncolysis induced tumor-specific immunity, and IL-24 production further developed effective responses.

A previous study has been demonstrated that IL-24 induces increase in the secretion of IL-6, TNF-α, and IFN-γ at high levels and trace amounts of GM-CSF, IL-2, IL-4, and lL-10[39]. In this study, we found that VG9-IL-24 treatment upregulated some cytokines that recruited and activated components of the immune system, especially increasing IFN-γ production significantly. As a proinflammatory cytokine, IFN-γ is important for immunity against intracellular pathogens, including vaccinia virus. VG9-IL-24 treatment produced elevated levels of IFN-γ, followed by recruitment of cells of the innate immune system to the inflamed tumor site, thus creating a proinflammatory environment, which attribute to the inhibition of growth and regression of the tumor. A previous study revealed that IL-24 administration enhanced serum IFN-γ levels and increased the number of IFN-γ-producing $CD8^+$ T cells in the spleen, thus enhancing $CD8^+$ T-cell cytotoxicity in CRC[40]. Therefore, VG9-IL-24 may stimulate systemic immunity through secondary induction of systemic antitumoral immunity mediated by IL-24.

It is notable that the oncolytic vaccinia virus VG9-IL-24 eradicated not only the primary tumor but also distant tumors. Such "bystander antitumor" activity may contribute to multiple mechanisms. First, as a secreted cytokine, IL-24 is able to interact with its cognate IL-20/IL-22 receptors that activate signal transduction pathways mediating antitumor activity[41]. In addition, vaccinia virus entered into the circulation, targeted and replicated at distant tumor sites, which directly destroyed distant tumors. IL-24 protein generated by VG9-IL-24 replication could also reach distant tumor sites to exert apoptosis induction, immune stimulation, and angiogenesis inhibition. Another potential mechanism is that VG9-IL-24 stimulated the immune system. VG9-IL-24 infection induced tumor-specific immunity and stimulated various immune cytokines, which activated antigen-presenting cells to present tumor antigens, thereby triggering an antitumor immune response. These possible mechanisms for "bystander antitumor" activity may support using vaccinia virus to produce constant IL-24 not only in situ but also systemically, therefore promoting antitumor efficiency in a local organ as well as metastases.

Collectively, we here constructed an oncolytic vaccinia virus armed with IL-24 named VG9-IL-24, which can act both as an oncolytic agent and as a vehicle for IL-24 gene transfer. Our results showed the potent antitumor effects of VG9-IL-24 on various CRC cell lines and in both human and murine CRC models. VG9-IL-24 may exert its excellent antitumor properties via multiple pathways including direct viral lytic effects, apoptosis induction, inhibition of angiogenesis, and stimulation of multiple antitumor immune responses. Our data indicated that IL-24 was a novel and multifunctional cancer-killing cytokine, which may present as a powerful tool for the noninvasive treatment of colorectal cancer.

ACKNOWLEDGMENTS: We are grateful to Professor Xinyuan Liu for providing the vaccinia shuttle plasmid (pCB) and the National Institutes for Food and Drug Control (NIFDC) for providing the vaccinia virus of Tian Tan strain VG9. This work was supported by grants from the National Natural Science Foundation of China (81703061), Innovation Capacity Development Plan of Jiangsu Province (BM2018023), Jiangsu Provincial Key Medical Discipline (ZDXKA2016017), Jiangsu Province Maternity and Child Health Project (FRC201741), Medical and Public Health Project of Wuxi Sci-Tech Development Fund (WX18IIAN027), and Wuxi Key Medical Talents (zdrc006). The authors declare no conflicts of interest.

REFERENCES

1. Gupta N, Kupfer SS, Davis AM. Colorectal cancer screening. JAMA 2019;321(20):2022–3.
2. Bell J, McFadden G. Viruses for tumor therapy. Cell Host Microbe 2014;15(3):260–5.

3. Guo ZS, Bartlett DL. Oncolytic viruses as platform for multimodal cancer therapeutics: A promising land. Cancer Gene Ther. 2014;21(7):261–3.
4. Fukuhara H, Ino Y, Todo T. Oncolytic virus therapy: A new era of cancer treatment at dawn. Cancer Sci. 2016;107(10):1373–9.
5. Eager RM, Nemunaitis J. Clinical development directions in oncolytic viral therapy. Cancer Gene Ther. 2011;18(5):305–17.
6. Kirn D, Martuza RL, Zwiebel J. Replication-selective virotherapy for cancer: Biological principles, risk management and future directions. Nat Med. 2001;7(7):781–7.
7. Everts B, van der Poel HG. Replication-selective oncolytic viruses in the treatment of cancer. Cancer Gene Ther. 2005;12(2):141–61.
8. Kaufman HL, Kohlhapp FJ, Zloza A. Oncolytic viruses: A new class of immunotherapy drugs. Nat Rev Drug Discov. 2015;14(9):642–62.
9. Hallden G, Portella G. Oncolytic virotherapy with modified adenoviruses and novel therapeutic targets. Expert Opin Ther Targets 2012;16(10):945–58.
10. Todo T. Oncolytic virus therapy using genetically engineered herpes simplex viruses. Front Biosci. 2008;13:2060–4.
11. Tayeb S, Zakay-Rones Z, Panet A. Therapeutic potential of oncolytic Newcastle disease virus: A critical review. Oncolytic Virother. 2015;4:49–62.
12. Haddad D. Genetically engineered vaccinia viruses as agents for cancer treatment, imaging, and transgene delivery. Front Oncol. 2017;7:96.
13. Yin L, Zhao C, Han J, Li Z, Zhen Y, Xiao R, Xu Z, Sun Y. Antitumor effects of oncolytic herpes simplex virus type 2 against colorectal cancer in vitro and in vivo. Ther Clin Risk Manag. 2017;13:117–30.
14. Silver J, Mei YF. Transduction and oncolytic profile of a potent replication-competent adenovirus 11p vector (RCAd11pGFP) in colon carcinoma cells. PLoS One 2011;6(3):e17532.
15. Eveno C, Mojica K, Ady JW, Thorek DL, Longo V, Belin LJ, Gholami S, Johnsen C, Zanzonico P, Chen N, Yu T, Szalay AA, Fong Y. Gene therapy using therapeutic and diagnostic recombinant oncolytic vaccinia virus GLV-1h153 for management of colorectal peritoneal carcinomatosis. Surgery 2015;157(2):331–7.
16. Foloppe J, Kintz J, Futin N, Findeli A, Cordier P, Schlesinger Y, Hoffmann C, Tosch C, Balloul JM, Erbs P. Targeted delivery of a suicide gene to human colorectal tumors by a conditionally replicating vaccinia virus. Gene Ther. 2008;15(20):1361–71.
17. Ziauddin MF, Guo ZS, O'Malley ME, Austin F, Popovic PJ, Kavanagh MA, Li J, Sathaiah M, Thirunavukarasu P, Fang B, Lee YJ, Bartlett DL. TRAIL gene-armed oncolytic poxvirus and oxaliplatin can work synergistically against colorectal cancer. Gene Ther. 2010;17(4):550–9.
18. Kirn DH, Wang Y, Le Boeuf F, Bell J, Thorne SH. Targeting of interferon-beta to produce a specific, multi-mechanistic oncolytic vaccinia virus. PLoS Med. 2007;4(12):e353.
19. Lee JH, Roh MS, Lee YK, Kim MK, Han JY, Park BH, Trown P, Kirn DH, Hwang TH. Oncolytic and immunostimulatory efficacy of a targeted oncolytic poxvirus expressing human GM-CSF following intravenous administration in a rabbit tumor model. Cancer Gene Ther. 2010; 17(2):73–9.
20. Deng L, Fan J, Guo M, Huang B. Oncolytic and immunologic cancer therapy with GM-CSF-armed vaccinia virus of Tian Tan strain Guang9. Cancer Lett. 2016;372(2): 251–7.
21. Menezes ME, Bhatia S, Bhoopathi P, Das SK, Emdad L, Dasgupta S, Dent P, Wang XY, Sarkar D, Fisher PB. MDA-7/IL-24: Multifunctional cancer killing cytokine. Adv Exp Med Biol. 2014;818:127–53.
22. Deng L, Fan J, Ding Y, Zhang J, Zhou B, Zhang Y, Huang B. Oncolytic efficacy of thymidine kinase-deleted vaccinia virus strain Guang9. Oncotarget 2017;8(25):40533–43.
23. O'Reilly MS, Boehm T, Shing Y, Fukai N, Vasios G, Lane WS, Flynn E, Birkhead JR, Olsen BR, Folkman J. Endostatin: An endogenous inhibitor of angiogenesis and tumor growth. Cell 1997;88(2):277–85.
24. Gupta P, Su ZZ, Lebedeva IV, Sarkar D, Sauane M, Emdad L, Bachelor MA, Grant S, Curiel DT, Dent P, Fisher PB. mda-7/IL-24: Multifunctional cancer-specific apoptosis-inducing cytokine. Pharmacol Ther. 2006;111(3):596–628.
25. Mhashilkar AM, Schrock RD, Hindi M, Liao J, Sieger K, Kourouma F, Zou-Yang XH, Onishi E, Takh O, Vedvick TS, Fanger G, Stewart L, Watson GJ, Snary D, Fisher PB, Saeki T, Roth JA, Ramesh R, Chada S. Melanoma differentiation associated gene-7 (mda-7): A novel anti-tumor gene for cancer gene therapy. Mol Med. 2001;7(4):271–82.
26. Su ZZ, Lebedeva IV, Sarkar D, Gopalkrishnan RV, Sauane M, Sigmon C, Yacoub A, Valerie K, Dent P, Fisher PB. Melanoma differentiation associated gene-7, mda-7/IL-24, selectively induces growth suppression, apoptosis and radiosensitization in malignant gliomas in a p53-independent manner. Oncogene 2003;22(8):1164–80.
27. Lebedeva IV, Su ZZ, Chang Y, Kitada S, Reed JC, Fisher PB. The cancer growth suppressing gene mda-7 induces apoptosis selectively in human melanoma cells. Oncogene 2002;21(5):708–18.
28. Lebedeva IV, Sarkar D, Su ZZ, Kitada S, Dent P, Stein CA, Reed JC, Fisher PB. Bcl-2 and Bcl-x(L) differentially protect human prostate cancer cells from induction of apoptosis by melanoma differentiation associated gene-7, mda-7/IL-24. Oncogene 2003;22(54):8758–73.
29. Pataer A, Vorburger SA, Barber GN, Chada S, Mhashilkar AM, Zou-Yang H, Stewart AL, Balachandran S, Roth JA, Hunt KK, Swisher SG. Adenoviral transfer of the melanoma differentiation-associated gene 7 (mda7) induces apoptosis of lung cancer cells via up-regulation of the double-stranded RNA-dependent protein kinase (PKR). Cancer Res. 2002;62(8):2239–43.
30. Pataer A, Vorburger SA, Chada S, Balachandran S, Barber GN, Roth JA, Hunt KK, Swisher SG. Melanoma differentiation-associated gene-7 protein physically associates with the double-stranded RNA-activated protein kinase PKR. Mol Ther. 2005;11(5):717–23.
31. Sun Y, Liu WZ, Liu T, Feng X, Yang N, Zhou HF. Signaling pathway of MAPK/ERK in cell proliferation, differentiation, migration, senescence and apoptosis. J Recept Signal Transduct Res. 2015;35(6):600–4.
32. Liu J, Chang F, Li F, Fu H, Wang J, Zhang S, Zhao J, Yin D. Palmitate promotes autophagy and apoptosis through ROS-dependent JNK and p38 MAPK. Biochem Biophys Res Commun. 2015;463(3):262–7.
33. Zuo G, Ren X, Qian X, Ye P, Luo J, Gao X, Zhang J, Chen S. Inhibition of JNK and p38 MAPK-mediated inflammation and apoptosis by ivabradine improves cardiac function in streptozotocin-induced diabetic cardiomyopathy. J Cell Physiol. 2019;234(2):1925–36.

34. Kitazumi I, Tsukahara M. Regulation of DNA fragmentation: The role of caspases and phosphorylation. FEBS J. 2011;278(3):427–41.
35. Sarkar D, Su ZZ, Lebedeva IV, Sauane M, Gopalkrishnan RV, Valerie K, Dent P, Fisher PB. mda-7 (IL-24) Mediates selective apoptosis in human melanoma cells by inducing the coordinated overexpression of the GADD family of genes by means of p38 MAPK. Proc Natl Acad Sci USA 2002;99(15):10054–9.
36. Duncan SA, Zhong Z, Wen Z, Darnell JE, Jr. STAT signaling is active during early mammalian development. Dev Dyn. 1997;208(2):190–8.
37. Frumovitz M, Sood AK. Vascular endothelial growth factor (VEGF) pathway as a therapeutic target in gynecologic malignancies. Gynecol Oncol. 2007;104(3):768–78.
38. Ramesh R, Mhashilkar AM, Tanaka F, Saito Y, Branch CD, Sieger K, Mumm JB, Stewart AL, Boquoi A, Dumoutier L, Grimm EA, Renauld JC, Kotenko S, Chada S. Melanoma differentiation-associated gene 7/interleukin (IL)-24 is a novel ligand that regulates angiogenesis via the IL-22 receptor. Cancer Res. 2003;63(16):5105–13.
39. Caudell EG, Mumm JB, Poindexter N, Ekmekcioglu S, Mhashilkar AM, Yang XH, Retter MW, Hill P, Chada S, Grimm EA. The protein product of the tumor suppressor gene, melanoma differentiation-associated gene 7, exhibits immunostimulatory activity and is designated IL-24. J Immunol. 2002;168(12):6041–6.
40. Ma YF, Ren Y, Wu CJ, Zhao XH, Xu H, Wu DZ, Xu J, Zhang XL, Ji Y. Interleukin (IL)-24 transforms the tumor microenvironment and induces anticancer immunity in a murine model of colon cancer. Mol Immunol. 2016;75:11–20.
41. Chada S, Mhashilkar AM, Ramesh R, Mumm JB, Sutton RB, Bocangel D, Zheng M, Grimm EA, Ekmekcioglu S. Bystander activity of Ad-mda7: Human MDA-7 protein kills melanoma cells via an IL-20 receptor-dependent but STAT3-independent mechanism. Mol Ther. 2004;10(6):1085–95.